

# Assessing Tissue Heterogeneity by non-Gaussian Measures in a Permeable Environment

1<sup>st</sup> Lorenza Brusini  
*Department of Computer Science*  
*University of Verona*  
 Verona, Italy  
 lorenza.brusini@univr.it

2<sup>nd</sup> Gloria Menegaz  
*Department of Computer Science*  
*University of Verona*  
 Verona, Italy  
 gloria.menegaz@univr.it

3<sup>rd</sup> Markus Nilsson  
*Department of Clinical Sciences*  
*Lund University*  
 Lund, Sweden  
 markus.nilsson@med.lu.se

**Abstract**—In diffusion MRI, the deviation of the Ensemble Average Propagator (EAP) from Gaussianity conveys information about the microstructural heterogeneity within an imaging voxel. Different measures have been proposed for assessing this heterogeneity. This paper assesses the performance of the Diffusional Kurtosis Imaging (DKI) and Simple Harmonics Oscillator Reconstruction and Estimation (SHORE) approaches using Monte Carlo simulations of water diffusion within synthetic axons with a permeable myelin sheath. The aim was also to understand the impact of myelin features such as its number of wrappings and relaxation ( $T_2$ ) rate on MR-observable parameters. To this end, a substrate consisting of parallel cylinders coated by a multi-layer sheet was considered, and simulations were used to generate the synthetic diffusion-weighted signal. Results show that myelin features affects the parameters quantified by both DKI and SHORE. A strong agreement was found between DKI and SHORE parameters, highlighting the consistency of the methods in characterising the diffusion-weighted signal.

**Index Terms**— $T_2$ -weighting, SHORE, DKI, Non Gaussianity, Kurtosis

## I. INTRODUCTION

Diffusion Magnetic Resonance Imaging (dMRI) has proved to be sensitive to microstructural changes. In order to interpret changes in dMRI metrics observed in both healthy development and disease, it is useful to consider microstructure modelling of the tissue. In the white matter of the brain, at least three compartments need to be considered: intra axonal, extra axonal, and myelin. The richness of lipids in the myelin sheath, however, leads to an overall  $T_2$  relaxation time that is much shorter in white compared to gray matter [1]. Due to its short  $T_2$  relaxation, the myelin water itself is assumed to contribute negligibly to the diffusion-weighted signal. However, myelin is altered in some cases such as the developing brain or diseases [2], [3] and exchange between the intra- and the extra-axonal compartments may take place through myelin, modifying the dMRI signal [4], [5]. Recently, an increasing interest has been devoted to the  $T_2$  relaxation time in the context of dMRI modelling. For example, Dortch et al. [6] administrated Chromium in the rat brain and, based on the assumption that this substance cannot enter the axon, modifications of the  $T_2$  spectrum suggested a longer relaxation time of the intra-axonal space. Veraart et al. [7] employed a model combining diffusion and  $T_2$  relaxation combined with an acquisition featuring multiple echo time (TE) and the estimated different

$T_2$  relaxation times in the different tissue compartments. The relationship between  $T_2$  and water exchange has also been investigated. In particular, Levesque and Pike [8] performed pathology-inspired analyses on simulations representing increased exchange following disease. They found that myelin water fractions and  $T_2$  values decreased for greater exchange concluding that myelin water fractions could be incorrectly related to changes in myelin content. Harkins et al. [9] also studied this relationship and found a linear correlation between the  $T_2$  profile and water volume fractions as measured by histological studies of rat spinal cord. They nevertheless found an overestimation of water fractions that could be reasonably attributed to exchange.

The impact of the heterogeneous environment within an imaging voxel can be captured by a number of different methods. While a homogeneous liquid has Gaussian diffusion, a heterogeneous environment express non-Gaussian diffusion. This Non Gaussianity (NG) can be captured, for example, by Diffusional Kurtosis Imaging (DKI) [10], which defines the deviation from Gaussian diffusion through the Diffusional Kurtosis. In this work, we study the kurtosis radial to a axon-like cylinder structure (RK). We also study the Simple Harmonic Oscillator based Reconstruction and Estimation (SHORE) method, which yield a so-called NG index [11] as a measure of the dissimilarity between the reconstructed propagator and its Gaussian part. In this paper, we aim at assessing both DKI and SHORE indices in the specific case of synthetic axons wrapped by myelin.

In this work, we investigate whether modulations of the diffusion process in synthetic axons due to different configurations of the myelin sheath can be captured by measures from DKI and SHORE. We thus aim to observe the sensitivity in the diffusion-weighted signal to myelin structure and especially to its multi-wrappings nature depending and its  $T_2$  relaxation time.

## II. METHODS

The simulation substrate comprised axon, myelin and extracellular compartments. Simulated particles moved freely in the xy-plane in the intra- and extra-axonal spaces, while their movements in myelin were confined to a one-dimensional spiralling compartment. The length of the spiral was computed

from the desired number of myelin wraps and the axon diameter. Particles were allowed to enter or leave the spiral at two specific points on the intra- and extra-axonal interfaces. Diffusion-weighting was simulated assuming a pulsed gradient setup with encoding time  $\delta = 15$  ms and diffusion time  $\Delta = 25$  ms. 100 equally spaced b-values in the range  $0 - 2500$  s/mm<sup>2</sup> were simulated. The time spent in each compartment ( $T_m$ ,  $m = A, M, E$ ) was also tracked to allow for compartment-specific relaxation times ( $T_{2,m}$ ) [12]. The simulated signal was given by

$$S = \frac{1}{K} \sum_{k=1}^K \exp(-i\phi_k) \sum_{m=A,M,E} \exp(-(T_m)_k/T_{2,m}). \quad (1)$$

where  $K$  was the number of particles,  $i^2 = -1$  and  $\phi_k$  was the phase information accrued by each particle due to the diffusion sensitising gradients.

The impact of simulation geometry on the simulated signal was explored by varying the number of wraps ( $n_{\text{wraps}} = 1, 2, 4, 8, 16, 32$ ) and the axon diameter ( $d_{\text{inner}} = 1, 2$   $\mu\text{m}$ ). For each simulation geometry two different myelin  $T_2$  relaxation times were considered for the myelin compartment: short ( $T_2 = 15$  ms) and long ( $T_2 = 85$  ms). Intra- and extra-axonal  $T_2$  were kept at 85 ms [12].

The simulated signals were then analysed by DKI [10] and by one dimensional SHORE [11] and each outcome was evaluated by computing the average mean squared error (MSE). Using DKI, the radial diffusivity (RD) and the RK were obtained by nonlinear estimation using the following equation:

$$S(b) = S_0 \cdot \exp \left[ -b \cdot RD + (b \cdot RD)^2 RK/6 \right] \quad (2)$$

where  $S_0$  was the signal without diffusion encoding. The one dimensional SHORE model was implemented as described in [11]:

$$S(q) = \sum_{n=0}^{N-1} \tilde{a}_n \phi_n(u, q) \quad (3)$$

with

$$\phi_n(u, q) = \frac{i^{-n}}{\sqrt{2^n n!}} \exp(-2\pi^2 q^2 u^2) H_n(2\pi u q) \quad (4)$$

where  $N$  was the radial order (in these experiments set to 6 [11]),  $\tilde{a}_n$  were the coefficients derived by fitting via quadratic programming,  $\phi_n(u, q)$  were the basis functions,  $u$  was a scaling parameter,  $H_n(2\pi u q)$  was the  $n$ th order Hermite polynomial and  $q = \sqrt{b/(\Delta - \delta/3)}$ . After the normalization of the coefficients:

$$a_n = \frac{\tilde{a}_n}{S_0} \quad (5)$$

where

$$S_0 = \sum_{n=0,2,4,\dots}^{N-1} \frac{\sqrt{n!}}{n!!} \tilde{a}_n, \quad (6)$$

the NG was subsequently computed for the one dimensional case as:

$$NG = \sqrt{1 - \left( \frac{a_0}{\sqrt{\sum_{n=0}^{n_{max}} a_n^2}} \right)^2} \quad (7)$$

where  $a_0$  corresponded to the Gaussian contribution of the diffusion signal.

Finally, the apparent fiber density (AFD) was also reported as the diffusion signal value at the highest b-value (here 2500 s/mm<sup>2</sup>) [13].

The correlation between each DKI estimated parameter and NG was quantified by computing the Spearman's rank correlation coefficient.

### III. RESULTS

In Fig. 1 we show the signal obtained by simulating diffusion in the substrate with different values of the parameters that are number of myelin wraps, myelin  $T_2$  relaxation and axonal inner diameter. The trends highlight a better differentiation across number of spiral layers in case of long myelin  $T_2$  and small axons.

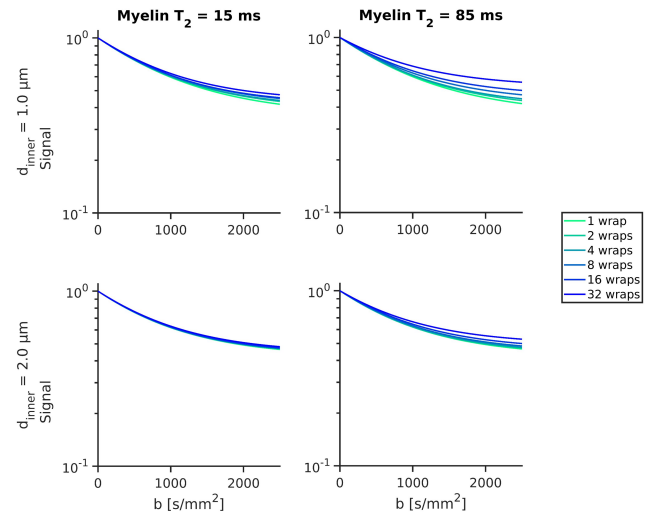


Fig. 1: Diffusion signal simulations varying the number of myelin wraps (colors), myelin  $T_2$  time (columns) and axon diameter (rows).

The fitting performance of the SHORE and DKI models in the considered conditions are reported in Fig. 2. Both the models reconstruct the signal with high accuracy. The average MSE was  $\text{MSE} = \sim 1.23 \exp(-05)$  for DKI fitting and  $\text{MSE} = \sim 1.91 \exp(-05)$  for SHORE. The fitting reflects the difference in myelin  $T_2$  relaxation when the number of wraps increases over 8 and for small axon diameters (below  $\mu\text{m}$ ).

Fig. 3 illustrates NG estimated with SHORE model and RK estimated with DKI model as a function of the number of myelin turns. Generally, NG increases in the range  $0.22 - 0.30$  showing a steeper slope of the curves for longer myelin

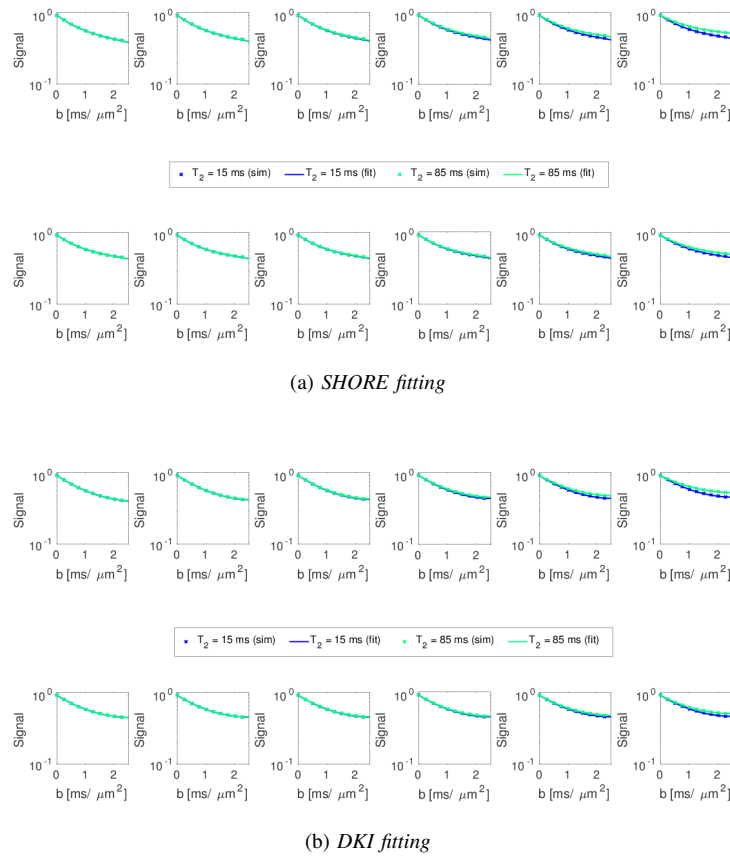


Fig. 2: Goodness of fit. The simulated and fitted diffusion signal were represented through crosses and solid line respectively. First row: axon diameter =  $1.0 \mu\text{m}$ ; second row: axon diameter =  $2.0 \mu\text{m}$ . Columns from one to six were representative of increasing number of wraps ( $n_{\text{wraps}} = 1, 2, 4, 8, 16, 32$ ). The myelin  $T_2$  was represented via different color: blue for  $T_2 = 15$  ms and light blue for  $T_2 = 85$  ms.

$T_2$  relaxation. RK shares the same trend as NG but covers a different range of values varying between 1.75 and 2.67.

Fig. 4 reports the estimated RD and AFD. RD follows a complementary behaviour when compared to NG and RK in Fig. 3, while AFD has the same trend. The range of variations were  $0.62-0.46 \mu\text{m}^2/\text{ms}$  and  $0.42-0.56$  for the two measures, respectively. Similar considerations as for NG and RK apply to RD and AFD with respect to  $T_2$  and number of wraps.

Fig. 5 shows the correlation between NG and each DKI index through scatter diagrams together with the respective Spearman's rank correlation coefficient and  $p$ -value. All the correlations resulted highly significant with  $p$ -value  $p < 0.001$ , with the highest value reached by NG and RK ( $r_S = 0.9748$ ).

#### IV. DISCUSSION

This work investigated the performance of indices calculated from SHORE and DKI models in reconstructing dMRI signal from permeable pores depending on myelin structure and  $T_2$ .

The signal curves show a faster decay for small axons with low number of myelin wraps. Moreover, small axons appear less affected by short  $T_2$  relaxation. We hypothesize that signal

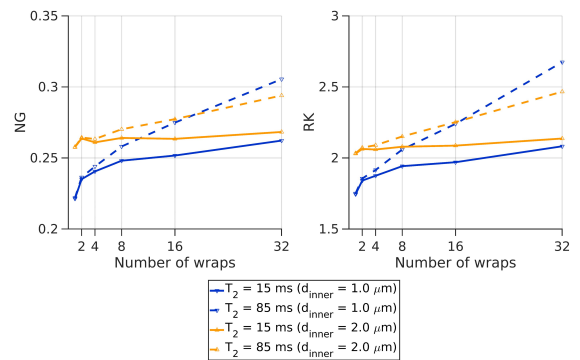


Fig. 3: SHORE model estimated Non Gaussianity (NG) and DKI model estimated radial kurtosis (RK) parameters in case of axon diameter  $1.0$  and  $2.0 \mu\text{m}$  and short (solid line) and long (dashed line) myelin  $T_2$  relaxation.

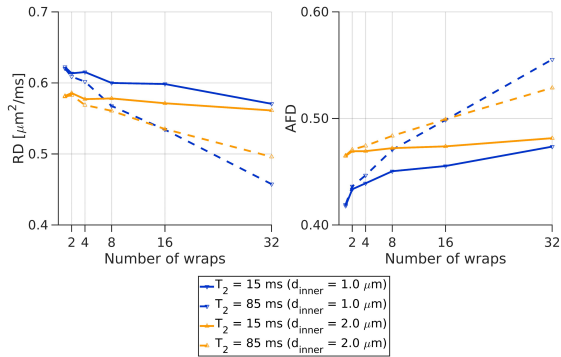


Fig. 4: DKI model estimated radial diffusivity (RD) and apparent fiber density (AFD) parameters in case of axon diameter 1.0 and 2.0  $\mu\text{m}$  and short (solid line) and long (dashed line) myelin  $T_2$  relaxation.

decays faster in smaller axons with respect to larger axons because the exchange rate is higher since a larger number of spins succeed in leaving the axon. We suggest also that signal decay decreases in both cases of axon diameter for increasing number of wraps because spins are increasingly more trapped in the myelin sheets and do not contribute to the diffusion signal unless  $T_2$  grows sufficiently, making the signal decay in myelin detectable in the given observation conditions. Consequently, the impact of the number of sheets is higher for smaller axons due to the exchange rate that scales up with the diameter. Our results of higher decay for small axons with low number of myelin wraps are in agreement with Harkins and Does [12] observations according to which a slowly diffusing myelin (corresponding to high number of myelin wraps in this study) traps the signal in the multi-wrappings compartment. Our results support the assumption that the myelin contribution to the diffusion signal is negligible for short  $T_2$  relaxation, though highlighting that it could become noticeable for axon diameter below 1.0  $\mu\text{m}$ .

The SHORE and DKI derived non-Gaussianity indices appear sensitive to exchange through the myelin structure irrespectively from the myelin  $T_2$  relaxation in small axons and low number of myelin turns. Based on the performance equivalence showed by NG and RK, we hypothesize a perfect agreement between the two descriptors. The estimated values of the NG were in line with the findings on real data [11]. The trend and the range of values of RK were also in agreement with the results of Harkins and Does [12]. The NG and RK increase for larger  $T_2$  may be explained by the larger signal decay in myelin that makes the contribution of this compartment detectable. Long relaxation time affects the amount of spin leakage, and thus contributing in reducing the signal (decreasing the impact of restriction). We can thus suppose that despite the difference of values, NG and RK both map the heterogeneity of the diffusion environment here

represented by the complex myelin structure having different number of turns and consequently to the diffusional exchange between intra- and extra-axonal compartments as hypothesized in [11], [14].

Therefore, in this respect, the SHORE model appears to behave as the benchmark represented by DKI. More specifically, regarding the latter, the trend and the range of values of the derived RD were close to those found by Harkins and Does [12], while AFD estimates were close to the axon plus myelin volume fraction set in our experiments. This further confirmed the hypothesis of Raffelt et al. [13] of an approximately linear relationship between AFD and the intracellular volume fraction. Also for RD and AFD as for NG and RK, the difference in  $T_2$  relaxation did not affect the estimates for small axons and low number of myelin wraps highlighting the suitability of these two indices as non-Gaussianity measures.

The lower RD for larger axons further supports the hypothesis that the increase of NG and RK for larger diameter is due to the dominant process of restriction. In fact, since the exchange rate decreases for bigger axon diameters, a smaller number of spins succeed in leaving the axon making the effect of restriction prominent. Conversely, the spin leakage is higher for smaller axons, resulting in an apparent higher RD and, consistently, smaller NG and RK. The significant correlations between indices confirms the strict relationship between each other.

## V. CONCLUSION

Both DKI and SHORE were sensitive to microstructure heterogeneity and were able of capturing it through a non-Gaussianity index. The sensitivity to the myelin structure was, however, lower for short  $T_2$ -relaxation time, although still present for low numbers of wraps. The sensitivity to tissue heterogeneity and to its changes with myelin structure has a strong translational potential in the definition of numerical biomarkers for demyelinating diseases such as multiple sclerosis.

## REFERENCES

- [1] T. Paus, D. Collins, A. Evans, G. Leonard, B. Pike, and A. Zijdenbos, "Maturation of white matter in the human brain: a review of magnetic resonance studies," *Brain research bulletin*, vol. 54, no. 3, pp. 255–266, 2001.
- [2] K.-J. Chang, S. A. Redmond, and J. R. Chan, "Remodeling myelination: implications for mechanisms of neural plasticity," *Nature neuroscience*, vol. 19, no. 2, p. 190, 2016.
- [3] M. Albert, J. Antel, W. Brück, and C. Stadelmann, "Extensive cortical remyelination in patients with chronic multiple sclerosis," *Brain Pathology*, vol. 17, no. 2, pp. 129–138, 2007.
- [4] M. Nilsson, J. Lätt, D. van Westen, S. Brockstedt, S. Lasič, F. Ståhlberg, and D. Topgaard, "Noninvasive mapping of water diffusional exchange in the human brain using filter-exchange imaging," *Magnetic resonance in medicine*, vol. 69, no. 6, pp. 1572–1580, 2013.
- [5] G. L. Nedjati-Gilani, T. Schneider, M. G. Hall, N. Cawley, I. Hill, O. Ciccarelli, I. Drobnjak, C. A. G. Wheeler-Kingshott, and D. C. Alexander, "Machine learning based compartment models with permeability for white matter microstructure imaging," *NeuroImage*, vol. 150, pp. 119–135, 2017.
- [6] R. D. Dortch, G. A. Apker, W. M. Valentine, B. Lai, and M. D. Does, "Compartment-specific enhancement of white matter and nerve ex vivo using chromium," *Magnetic resonance in medicine*, vol. 64, no. 3, pp. 688–697, 2010.

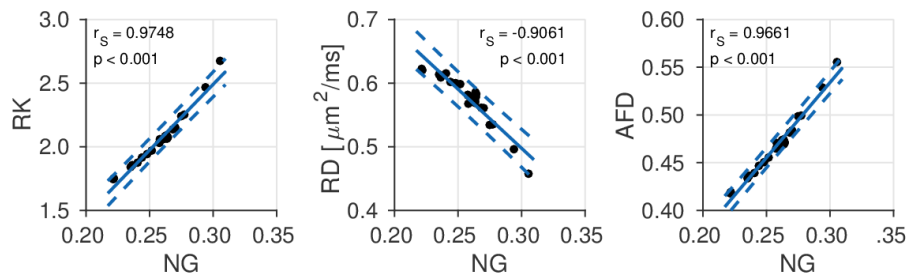


Fig. 5: Scatter diagrams for Non Gaussianity (NG) and radial kurtosis (RK), radial diffusivity (RD) and axonal fiber density (AFD) respectively. The Spearman's rank correlation coefficient is reported for each couple of indices with the respective  $p$ -value.

- [7] J. Veraart, D. S. Novikov, and E. Fieremans, "Te dependent diffusion imaging (teddi) distinguishes between compartmental t2 relaxation times," *Neuroimage*, 2017.
- [8] I. R. Levesque and G. B. Pike, "Characterizing healthy and diseased white matter using quantitative magnetization transfer and multicomponent t2 relaxometry: A unified view via a four-pool model," *Magnetic resonance in medicine*, vol. 62, no. 6, pp. 1487–1496, 2009.
- [9] K. D. Harkins, A. N. Dula, and M. D. Does, "Effect of intercompartmental water exchange on the apparent myelin water fraction in multi-exponential t2 measurements of rat spinal cord," *Magnetic resonance in medicine*, vol. 67, no. 3, pp. 793–800, 2012.
- [10] J. H. Jensen, J. A. Helpert, A. Ramani, H. Lu, and K. Kaczynski, "Diffusional kurtosis imaging: The quantification of non-gaussian water diffusion by means of magnetic resonance imaging," *Magnetic resonance in medicine*, vol. 53, no. 6, pp. 1432–1440, 2005.
- [11] E. Ozarslan, C. Koay, T. Shepherd, M. Komlosh, M. Irfanoglu, C. Pierpaoli, and P. Basser, "Mean apparent propagator (map) mri: A novel diffusion imaging method for mapping tissue microstructure," *NeuroImage*, vol. 78, pp. 16 – 32, 2013.
- [12] K. Harkins and M. Does, "Simulations on the influence of myelin water in diffusion-weighted imaging," *Physics in medicine and biology*, vol. 61, no. 13, p. 4729, 2016.
- [13] D. Raffelt, J.-D. Tournier, S. Rose, G. R. Ridgway, R. Henderson, S. Crozier, O. Salvado, and A. Connelly, "Apparent fibre density: a novel measure for the analysis of diffusion-weighted magnetic resonance images," *Neuroimage*, vol. 59, no. 4, pp. 3976–3994, 2012.
- [14] J. H. Jensen and J. A. Helpert, "Mri quantification of non-gaussian water diffusion by kurtosis analysis," *NMR in Biomedicine*, vol. 23, no. 7, pp. 698–710, 2010.